Ecological Modelling 285 (2014) 39–53

Contents lists available at ScienceDirect

Ecological Modelling

journal homepage: www.elsevier.com/locate/ecolmodel

Evaluating the impact of ocean acidification on fishery yields and profits: The example of red king crab in Bristol Bay

André E. Punt[a,*], Dusanka Poljak[a], Michael G. Dalton[b], Robert J. Foy[c]

[a] School of Aquatic and Fishery Sciences, Box 355020, University of Washington, Seattle, WA 98195, United States
[b] Alaska Fisheries Science Center, 7600 Sand Way Point Way, NE, Seattle, WA 98115, United States
[c] Alaska Fisheries Science Center, Kodiak Laboratory, 301 Research Ct, Kodiak, AK 99615, United States

ARTICLE INFO

Article history:
Received 28 November 2013
Received in revised form 12 April 2014
Accepted 16 April 2014
Available online 13 May 2014

Keywords:
MSY
MEY
North Pacific
Ocean acidification
Red king crab

ABSTRACT

A stage-structured pre-recruit model was developed to capture hypotheses regarding the impact of ocean acidification on the survival of pre-recruit crab. The model was parameterized using life history and survival data for red king crab (*Paralithodes camtschaticus*) derived from experiments conducted at the National Marine Fisheries Service Kodiak laboratory. A parameterized pre-recruit model was linked to a post-recruit population dynamics model for adult male red king crab in Bristol Bay, Alaska that included commercial fishery harvest. This coupled population dynamics model was integrated with a bioeconomic model of commercial fishing sector profits to forecast how the impacts of ocean acidification on the survival of pre-recruit red king crab will affect yields and profits for the Bristol Bay red king crab fishery for a scenario that includes future ocean pH levels predictions. Expected yields and profits were projected to decline over the next 50–100 years in this scenario given reductions in pre-recruit survival due to decreasing ocean pH levels over time. The target fishing mortality used to provide management advice based on the current harvest policy for Bristol Bay red king crab also declined over time in response to declining survival rates. However, the impacts of ocean acidification due to reduced pre-recruit survival on yield and profits are likely to be limited for the next 10–20 years, and its effects will likely be masked by natural variation in pre-recruit survival. This analysis is an initial step toward a fully integrated understanding of the impact of ocean acidification on fishery yields and profits, and could be used to focus future research efforts.

1. Introduction

The world's oceans are absorbing atmospheric carbon dioxide (CO_2) from burning fossil fuels, deforestation, cement production, and other human activities that contribute to climate change (Feely et al., 2004). The increase in oceanic CO_2 has caused an average decrease of surface ocean pH by 0.1 units from pre-industrial levels, the equivalent of a 30% increase in acidity, and global average pH in surface waters, now 8.1, is predicted to fall to 7.8 before 2100 in a standard climate scenario (Malakoff, 2012). This ocean acidification (OA), in addition to decreasing the pH, reduces the saturation of calcium carbonate, making it more difficult for some calcifying organisms to sequester calcium and carbonate to build shells. Unlike global warming which has a robust literature on impacts (see Sumaila et al. (2011) for a review of fisheries impacts), few studies have assessed the wider impacts of OA on human society. An important early study by Cooley and Doney (2009) focused mainly on future economic impacts (i.e., potential revenue losses) from OA for US mollusk production, and this sector has received the most attention. However, these studies do not differentiate OA effects on different life-history stages, and therefore, the same type of analysis cannot be applied to animals where demographic factors are a critical feature of population dynamics, which is true for many commercially-important species. In particular, commercially-important crab stocks in the waters off Alaska have complicated population dynamics and are susceptible to the physiological and ecological effects of OA.

The saturation horizon of calcium carbonate in the North Pacific Ocean is an order of magnitude shallower than in the North Atlantic (Doney et al., 2009). In the Bering Sea, waters below 40 m are seasonally undersaturated in aragonite while calcite saturation states are low (<2.0) below 50 m (Mathis et al., 2011). In the Arctic Region, OA effects on organisms and ecosystems are imminent with current

* Corresponding author. Tel.: +1 206 221 6319; fax: +1 206 685 7471.
E-mail addresses: aepunt@uw.edu, aepunt@u.washington.edu (A.E. Punt).

http://dx.doi.org/10.1016/j.ecolmodel.2014.04.017
0304-3800/

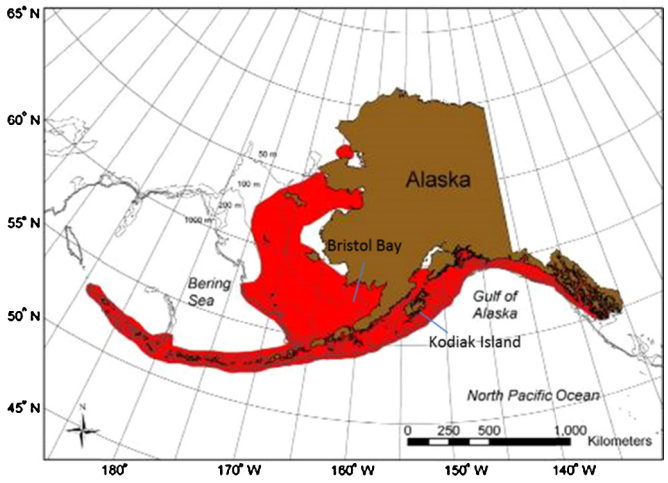

Fig. 1. Red king crab general distribution in the North Pacific Ocean, identifying the area of the largest stock in Bristol Bay in the eastern Bering Sea.

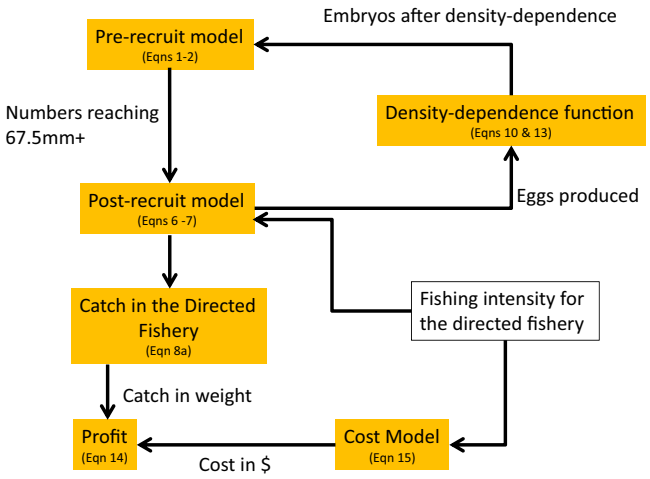

Fig. 2. Conceptual overview of the pre- and post-recruit models.

seasonal undersaturation in the surface waters (Fabry et al., 2009; Steinacher et al., 2009).

Bristol Bay red king crab (*Paralithodes camtschaticus*), BBRKC (see Fig. 1 for the distribution of BBRKC), inhabit waters less than 100 m as juveniles and adults. Larval stages of BBRKC are pelagic between 40 and 84 days followed by a transitional pelagic-epibenthic stage that lasts approximately 14 days depending on temperature and food availability (Kovatcheva et al., 2006; also see Weber, 1967 and Armstrong et al., 1981 for review). Bristol Bay red king crab are targeted by one of the largest crab fisheries in the Bering Sea and Aleutian Islands (BSAI) region of the North Pacific. In 2009–2011, the BBRKC fishery produced an annual average of a little more than eight and a half million pounds of finished products, and was estimated to have generated real (i.e., 2011 dollars) first-wholesale revenues of about one hundred fifteen million dollars per year (Garber-Yonts and Lee, 2012, Table 10).

The BBRKC fishery may be impacted in the future by OA as crab respond to the decreases in pH and decreased availability of calcium carbonate. Experiments conducted at the National Marine Fisheries Service (NMFS) Kodiak Laboratory in Kodiak, Alaska, concluded that although calcification rates in juvenile red king crab were not affected, survival rates decreased as a function of lower pH (Long et al., 2013a). Other studies on decapod crustaceans also found calcification rates not to be affected by ocean acidification (e.g. Kurihara et al., 2008; Ries et al., 2009) while higher mortality rates at juvenile stages were similarly found in other crab species (Ceballos-Osuna et al., 2013). A broader consideration of crustaceans found a range of responses presumed to be a function of physiological capacity to compensate for the changes in pH (Whiteley, 2011).

The BBRKC fishery is managed jointly by the North Pacific Fishery Management Council (NPFMC) and the State of Alaska. The federal assessment process for this species provides estimates of the Overfishing Limit (OFL, the level of catch corresponding to the proxy for the fishing mortality which achieves Maximum Sustainable Yield, MSY, F_{MSY}) and the Acceptable Biological Catch (ABC, a level of catch lower than the OFL to account for scientific uncertainty), while the State of Alaska sets the Total Allowable Catch (TAC). The OFL for BBRKC is currently based on a harvest control rule used for stocks for which stock biomass and $F_{35\%}$ (the fishing mortality rate in the directed fishery which reduces mature male-per-recruit to 35% of its unfished level) can be estimated, but there are no reliable estimates of F_{MSY} and corresponding biomass, B_{MSY} (NPFMC, 2008).

The stock assessments for BBRKC which are used to provide the estimates of biomass and productivity required to compute OFLs, ABCs and TACs are based on a statistical catch-at-length analysis technique (Punt et al., 2013). This technique (see Zheng and Siddeek, 2009, 2010, 2011 for applications to BBRKC) involves estimating the parameters of a length-, shell condition-, and sex-structured population dynamics model by fitting to catch, survey and fishery length–frequency data, and survey indices of abundance.

In this paper, we develop an integrated bioeconomic model to estimate maximum sustainable yield (MSY) and maximum economic yield (MEY) for the BBRKC fishery, and evaluate how these quantities change over time in response to the physiological impact of OA (see Fig. 2 for a conceptual overview of the model and how the projections are undertaken). The integrated bioeconomic model consists of three components: (a) a pre-recruit model which models red king crab from the embryo stage to the length at which they are included in the models used for providing management advice, (b) a model of post-recruit crab which includes the impact of the directed fishery for red king crab and a trawl fishery which incidentally takes red king crab, and (c) a model of profits for the commercial fishing sector arising from red king crab harvesting. The combined bioeconomic model is used then to forecast the relationship between yield and profit over time, and hence that between MSY and MEY over time.

2. Methods

2.1. The pre-recruit model

A stage-structured population model was used to forecast the changes over time in recruitment to the first length-class in the post-recruit model (67.5 mm carapace length, CL; Zheng and Siddeek, 2010):

$$\underline{N}_{T+t+1} = \mathbf{G}_T \Omega_T \underline{N}_{T+t} \quad (1)$$

where $\underline{N}_{T+t}$ is the vector of numbers-at-stage at time $T+t$ (all embryos enter the first stage when they are spawned), $\mathbf{G}_T$ is the transition matrix (i.e. the matrix of probabilities of growing from one stage to each other stage for embryos spawned at time T; consistent with assessments for most crustaceans, the matrix $\mathbf{G}$ is assumed to be lower triangular, reflecting the assumption that very few animals shrink following molting), and Ω_T is the survival matrix for embryos spawned at time T. The survival and growth rates for animals spawned at time T over their time as pre-recruits are set to those calculated for time T. This is an adequate approximation

Table 1
Stage durations for Bristol Bay red king crab.

Stage	Duration [Average] (days)	Minimum time spent in stage (days)	Molts	CL (mm)	Source
Z1–Z4	10–14 [12]	10	1	1.18–2.07	Kovatcheva et al. (2006)
G	18–56 [37]	18	1	1.8–2.0	Kovatcheva et al. (2006)
C1–C8	20–30 [25]	20	1	2.18–9.5	Donaldson et al. (1992)
J1	365 [365]	365	3	9–22	Loher et al. (2001)
J2	365 [365]	365	2	23–46	Loher et al. (2001)
J3–J4	365 [365]	365	1	47–62	Loher et al. (2001)
J5	174 [174]	174	1	63–67.5	Loher et al. (2001)

given the slow change over time in pH relative to the duration of the pre-recruit stage for BBRKC. The last stage in this model is the first length-class in the post-recruit model.

The pre-recruit model considers 18 pre-recruit stages (4 zoeal stages, 1 glaucothoe stage, and 13 pre-recruit stages, denoted Z1–Z4, G, C1–C8, and J1–J5). The stages with the shortest durations, the zoeal stages, last on average 12 days (Table 1). The time-step for the model [6 days] is set to half of the average zoeal stage duration. It is assumed that all individuals within a stage are subject to the same survival probability and stage duration, and that individuals must stay in a stage for a defined minimum amount of time before progressing to the next stage (the ages-within-stages approach to constructing stage-structured models) (Table 1; Kovatcheva et al., 2006). This is achieved by dividing each of the 18 stages into sub-stages where the number of sub-stages is one plus the number of time-steps that an animal needs to remain in a stage. Ocean acidification is assumed to impact all pre-recruit stages even though experimental evidence to date is based on the juvenile (C1–C8 and J1–J5) stages.

The matrix $\mathbf{G}_T\Omega_T$ determines the combined effects of growth and mortality. This matrix can be written as:

$$\mathbf{G_T\Omega_T} = \begin{array}{c} \begin{matrix} (- \text{ From } -) & (- \text{ From } -) & \text{(From)} \\ (- \text{ Stage1 } -) & (- \text{ Stage2 } -) & \text{(Stages 3+)} \end{matrix} \\ \begin{pmatrix} 0 & 0 & 0 & 0 & 0 & \ldots \\ S_{1,T} & S_{1,T}(1-P_{1,T}) & 0 & 0 & 0 & \ldots \\ 0 & S_{1,T}P_{1,T} & 0 & 0 & 0 & \ldots. \\ 0 & 0 & S_{2,T} & 0 & 0 & \ldots \\ 0 & 0 & 0 & S_{2,T} & S_{2,T}(1-P_{2,T}) & \ldots \\ 0 & 0 & 0 & 0 & S_{2,T}P_{2,T} & \ldots \\ 0 & 0 & 0 & 0 & 0 & \ldots \\ \ldots & \ldots & \ldots & \ldots & \ldots & \ldots \end{pmatrix} \end{array} \quad (2)$$

for the case in which animals must stay at least one time-step in stage 1 and two time-steps in stage 2. $S_{i,T}$ is the probability of survival for stage i for animals spawned at time T, and $P_{i,T}$, is the probability of growing out of stage i for animals spawned at time T.

The values for the $S_{i,T}$ and $P_{i,T}$ are solved to match values for expected survival ($\tilde{S}_{i,T}$) for stage i for embryos spawned at time T and the non-OA-impacted expected stage duration ($\tilde{d}_i$). The predicted values for $\tilde{S}_{i,T}$ and $\tilde{d}_i$ for a stage with n sub-stages are (Appendix A):

$$\tilde{S}_{i,T} = \frac{S_{i,T}^n P_{i,T}}{1 - S_{i,T}(1-P_{i,T})}; \quad \tilde{d}_i = \frac{\sum_{y=T}^{T+tt}(y+1)x_{i,y}S_{i,T}P_{i,T}}{\sum_{y=T}^{T+tt}x_{i,y}S_{i,T}P_{i,T}} \quad (3)$$

where $x_{i,y}$ is the number of animals leaving stage i at time step y (for stage 1, this would be the numbers entering class 3 in Eq. (2)), and tt is the total number of time steps ($tt \sim 1100$).

Survival rates for each pH level are calculated based on a power function relationship between ocean pH and survival rate which was selected as a likely form which might be able to mimic the data on the relationship between survival and pH from Long et al. (2013a):

$$\tilde{S}_{i,T} = \tilde{S}_i \left(1 - \gamma \left\{ \frac{|\text{pH}_T - \text{pH}|}{\text{pH}} \right\}^{\phi_S} \right) \quad (4)$$

where, $\tilde{S}_{i,T}$ is the survival rate for animals in stage i that were spawned at time T, $\tilde{S}_i$ is the reference (non-OA impacted) survival rate for stage i, and γ are ϕ_S are the parameters of the relationship, pH is the reference (OA-neutral) pH value (8.1), and pH_T is the ocean pH at time T. Results are shown for linear ($\phi_S = 0$; γ estimated) and non-linear (ϕ_S and γ estimated) versions of Eq. (4). The linear formulation was selected because it parsimonious which might be appropriate given the relatively small number of crab included in the experiments conducted by Long et al. (2013a).

A simple approximation to a standard OA scenario with changes over time in pH was calculated using the straight line that joins the predictions of average global pH levels in oceans between 2000 and 2200; $\text{pH}_{2000} = 8.1$, $\text{pH}_{2200} = 7.4$ (Hall-Spencer et al., 2008; Caldeira and Wickett, 2003).

Experimental data on the impact of pH on survival of juvenile red king crab from Long et al. (2013a) were used to estimate the long term relationship between ocean pH and red king crab survival rate. The experiment involved two treatments (pH = 7.8 and 7.5) and one control (pH = 8.0). The treatment levels in the experiment correspond (approximately) to the environmental conditions expected to be encountered by embryos spawned in 2088 and 2159 in our simple OA scenario. In the experiment, ninety red king crabs were randomly assigned to three tanks, with 30 crabs per tank, and the tanks were randomly assigned one of the two treatments or the control. The total experimental duration for each treatment level was 192 days, after which the time between moltings became too long (~1 year).

The expected stage survivals ($\tilde{S}_i$) in the absence of OA impacts were selected given the overall expected survival ($SS = 0.0000046$)[1] from embryo to subsequent recruitment inferred from the stock assessment (Zheng and Siddeek, 2010), where the survival rate for the stages covered by the experiment (C1–C8) were tuned to equal the survival for the controls in the experiment. The survival rate for stage i was assumed to depend on the number of molts during that stage (mt_i; Table 1), i.e., $\tilde{S}_i = e^{-\lambda mt_i}$ where the value of λ was set so that $SS = \prod_{i=1}^{18}\tilde{S}_i$, i.e. $\lambda = \ell nSS / \sum_{i=1}^{18} mt_i$.

The values for the parameters γ, and η_S (from Eq. (4)) were selected to best replicate the data from the NMFS Kodiak experiment. The calibration involved minimizing the following objective function:

$$\sum_i \sum_t \left(\frac{S_{i,t}^{obs} - \hat{S}_{i,t}}{S_{i,t}^{obs}} \right)^2 \quad (5)$$

[1] The average value over spawning years 1968–2004 of the ratio of the number of animals recruiting to the first size-class in the assessment model divided by the number of embryos spawned predicted from the stock assessment.

where $S_{i,t}^{obs}$ is the proportion of treated animals (7.8 and 7.5 pH respectively for $i = 1,2$) which were still alive after $6t$ days, and $\hat{S}_{i,t}$ is the proportion of animals entering stage J1 which survived $6t$ days based on the model. Days after which no animals were alive were omitted from Eq. (5). Uncertainty was accounted for using a bootstrap procedure. For each of the 100 bootstrap replicates, this involved randomly selecting (with replacement) animals from the control and each of the treatments and then fitting linear and non-linear models (see Eq. (4)) to each bootstrap data set. Confidence intervals for the parameters of the model and the model predictions were then determined using the percentile method (Efron, 1982).

2.2. Modeling post-recruit red king crab

The dynamics of the post-recruits (and hence the impacts of the fishery) are modeled using a population dynamics model which is a simplification of the current stock assessment model for BBRKC (Zheng and Siddeek, 2009, 2010, 2011) in which only males are modeled, fewer length-classes are used, and no consideration is taken of shell condition. This simplification was made for computational reasons, but will not impact the results markedly as the fishery is only allowed to retain males, and red king crab do not exhibit a terminal molt. Mature male biomass (MMB) at the time of mating (taken to be 15 February) is used as a proxy for fertilized egg production in this model, consistent with how management advice is provided for BSAI crab (NPFMC, 2008). The basic dynamics of the population in the model are:

$$\underline{N}_{y+1} = \mathbf{X}\mathbf{S}_y\underline{N}_y + \underline{R}_{y+1} \tag{6}$$

where $\underline{N}_y$ is the vector of numbers-at-stage (males only) at the start of year y, $\mathbf{X}$ is the transition matrix (assumed as before to be lower triangular), $\mathbf{S}_y$ is the survival matrix for year y, and $\underline{R}_y$ is the vector of recruits for year y. The matrix $\mathbf{S}_y$ is diagonal with elements:

$$S_{y,i,i} = e^{-M_y}\left(1 - J_i^T F_y^T\right)\left(1 - J_{y,i}^D F_y^D\right) \tag{7}$$

where M_y is the instantaneous rate of natural mortality for year y, J_i^T is selectivity due to trawl fishery bycatch on animals in length-class i, F_y^T is the exploitation rate due to the trawl fishery during year y, $J_{y,i}^D$ is selectivity for the directed fishery during year y on animals in length-class i, and F_y^D is the exploitation rate due to the directed fishery during year y. Bristol Bay red king crab have historically also been caught and discarded by the fishery for Eastern Bering Sea Tanner crab, but this source of mortality is ignored for the analyses of this paper because discard in the Tanner crab fishery has been low historically and very low in recent years. In model projections, F_y^T in Eq. (7) is set to the average over 2006–2011, while future selectivity in the directed and groundfish fishery is set to that for the most recent epoch (see Table B.1). Future values for F_y^D are determined by the scenario under consideration (see Section 2.4). There is a minimum size limit for the directed fishery so some crabs caught during the directed fishery are discarded. The retained and discarded catch (in mass) by the directed fishery during year y, $\tilde{C}_y^D$ and $\bar{C}_y^D$, are:

$$\tilde{C}_y^D = \sum_i Q_i w_i J_{y,i}^D F_y^D N_{y,i} e^{-0.5M_y} = \sum_i w_i \tilde{C}_{y,i}^D \tag{8a}$$

$$\bar{C}_y^D = \sum_i (1 - Q_i) w_i J_{y,i}^D F_y^D N_{y,i} e^{-0.5M_y} = \sum_i w_i \bar{C}_{y,i}^D \tag{8b}$$

where Q_i is the proportion of crab in length-class i which is retained, w_i is the average mass of a male crab in length-class i, $N_{y,i}$ are numbers of animals in length-class i at the start of year y, and the fishery is assumed to take place half way through the model year which start on 1 July.

The discard by the trawl fleet is computed under the assumption that the directed and trawl fisheries are sequential (the directed fishery has historically occurred over a very short interval whereas the trawl fishery occurs essentially throughout the year):

$$\bar{C}_y^T = \sum_i w_i J_{y,i}^T F_y^T N_{y,i} e^{-0.5M_y}(1 - J_{y,i}^D F_y^D) = \sum_i w_i \bar{C}_{y,i}^T \tag{9}$$

In principle, the trawl fishery could be modeled as occurring over the entire year rather than as pulse in the middle of the year. However, the catch by the trawl fishery is negligible compared to that by the directed fishery so this complication is ignored here.

Under the assumption that only the directed fishery occurs before mating, and that mating occurs on 15 February of year $y+1$, the mature male biomass for year y, MMB_y, is computed using the equation:

$$MMB_y = \sum_i N_{y,i} f_i e^{-0.75M_y}(1 - J_{y,i}^D F_y^D) \tag{10}$$

where f_i is the fecundity of a crab in length-class i. Density-dependence is assumed to impact the survival rate of embryos (see Eqs. (13a) and (13b)) and is modeled based on the mature male biomass at the time of mating for consistency with how management advice is provided and projections conducted for crab stocks in Bering Sea (NPFMC, 2008).

Recruitment only occurs to the first length-class in the model. Recruitment during future year y is calculated as the sum of the numbers recruiting during year y based on spawning during years y', where the spawning year ranges from 1 to 10 years before year y.

$$R_y = \phi \sum_{y'=y-10}^{y-1} f(MMB_{y'}) G(y', y) \tag{11}$$

where $G(y', y)$ is the fraction of animals which were spawned during year y' which recruit during year y. The matrix $\mathbf{G}$ is the link between the pre- and post-recruit models. The entries in this matrix are computed by projecting the pre-recruit model forward for embryos produced during year y' and recording the fraction of these embryos which survive to the stage corresponding to the first length-class in the post-recruit model in each future year. The entries of the matrix $\mathbf{G}$ depend on OA because OA impacts survival and growth in the pre-recruit model. The symbol ϕ in Eq. (11) is a constant, computed so that the population remains at its equilibrium unfished level in the absence of ocean acidification and exploitation ($F_y^D = F_y^T = 0$). To find the value of ϕ, R_y is set to 1, the resulting MMB is found, and $G(y', y)$ is set based on the pre-recruit model with no OA impact, i.e.:

$$\phi = \frac{1}{\sum_{y'=y-10}^{y-1} f(MMB_{y'}) G(y', y)} \tag{12}$$

where the number of animals entering the first stage of the pre-recruit model is governed by a Ricker (Eq. (13a)) or Beverton–Holt (Eq. (13b)) relationship, i.e.:

$$f(MMB_{y'}) = R_0 \frac{MMB_{y'}}{MMB_0} e^{(5/4)\ln(5h)(1-(MMB_{y'}/MMB_0))} e^{\varepsilon_y - \sigma_R^2/2} \tag{13a}$$

$$f(MMB_{y'}) = \frac{4hR_0 MMB_{y'}/MMB_0}{(1-h) + (5h-1)MMB_{y'}/MMB_0} e^{\varepsilon_y - \sigma_R^2/2} \tag{13b}$$

where MMB_y can be a historical or projected value, and $\varepsilon_y \sim N(0; \sigma_R^2)$ and σ_R is the standard deviation of the log-deviations about Eqs. (13a) and (13b). R_0 and MMB_0 are respectively the recruitment and mature male biomass in an unfished state and h is the 'steepness' of Eqs. (13a) and (13b) (the expected numbers entering the first stage of the pre-recruitment model when $MMB = 0.2MMB_0$, expressed as

a proportion of R_0; Francis (1992)). Eqs. (13a) and (13b) imply that density-dependence occurs at the embryo stage. However, the results are insensitive to density-dependence occurring at any stage during the pre-recruit phase.

The parameters of the model which are estimated by fitting it to the data collected from the fishery and during surveys are: (a) natural mortality, (b) the fully-selected fishing mortality for each year for the directed and trawl fisheries when the catch was non-zero (i.e., when the directed fishery was not closed), (c) the parameters which define the transition matrix, (d) selectivity-at-length for each fishery (potentially changing over time), (e) catchability and selectivity-at-length for male crab in two surveys (conducted by the NMFS and the Bering Sea Fishery Research Foundation) (again potentially changing over time), (f) the probability of being landed and retained given being caught in the directed pot fishery, (g) the probability of being retained in the directed pot fishery, (h) the initial length-structure of the population, (i) the mean recruitment, $\bar{R}$ and (j) the deviations in the recruitment about mean recruitment, ε_y, i.e. $R_y = \bar{R}e^{\varepsilon_y}$. Appendix B outlines the likelihood function which is maximized to obtain the values for the parameters of the post-recruit model. The values for fecundity- and weight-at-length are set based on the outcomes of auxiliary studies (Appendix B).

The parameters that determine historical changes over time in population abundance by length-class are not sensitive to the choice of the how density-dependence is modeled because the parameters of Eqs. (13a) and (13b) are estimated after the stock-assessment is conducted (Zheng and Siddeek, 2009, 2010, 2011; Punt et al., 2013). However, the values for h and R_0 differ between Eqs. (13a) and (13b) because they are chosen so that under deterministic considerations (i.e., $\sigma_R = 0$), $F_{MSY} = F_{35\%}$ and $B_{MSY} = B_{35\%}$ where the recruitment at $B_{35\%}$ is set to an average selected by the Scientific and Statistical Committee of the NPMFC (1995 to present) (NPFMC, 2008; Punt et al., 2013; Table B.5). The assumption that $F_{MSY} = F_{35\%}$ and $B_{MSY} = B_{35\%}$ is commonly made when conducting projections for North Pacific crab and groundfish stocks (e.g. Punt et al., 2012). Punt et al. (2014) show that the assumption $F_{MSY} = F_{35\%}$ is supported for several North Pacific crab stocks.

2.3. Computing profits and MEY

The profit (excluding fixed costs which do not affect MEY) during year y is given by:

$$\pi_y = (pC_y - V_y) \tag{14}$$

where p is price per kg (assumed to be time-invariant), and V_y is the variable cost during year y, calculated for the costs of fuel, food, and bait:

$$V_y = E_y c_F + E_y c_G + P_y^D c_b \tag{15}$$

where E_y is a sum of days fishing $\left(E_y^F\right)$ and days traveling $\left(E_y^T\right)$, and c_F, c_G and c_b are respectively the average daily costs of fuel and food, and bait cost per potlift (Table 2). The average price per kg was calculated from State of Alaska fish tickets for the years 2006–2010 as the ratio of total ex-vessel revenues (current dollars summed over 2006–2010) divided by total landings (crab weight in pounds summed over 2006–2010 and converted to kilograms). The average costs for fuel, food, and bait were calculated from values in the BSAI Crab Rationalization Program Economic Data Reports (EDRs) for the years 2006–2010. Fuel and bait costs for the Bristol Bay red king crab fishery were pro-rated after aggregating data for these costs over all crab fisheries reported in the EDRs to address concerns about data quality for cost elements collected at the level of individual crab fisheries. Fuel and food cost per day was calculated as the ratio of total fuel and food costs for 2006–2010 divided by the sum of days fishing and days traveling which were reported in the EDRs. Bait cost per pot lift was calculated as the ratio of total bait costs for 2006–2010 divided by the total number of potlifts, where the number of potlifts was taken from fish tickets.

Table 2
The values for economic parameters.

Price per kg	$10.88
Fuel cost per day,	$1548.19
Food cost per day	$125.79
Bait cost per pot lift	$6.30

The number of potlifts in the directed fishery during year y, P_y^D, is a linear function of days fishing, $P_y^D = 78.334E_y^F$, while days fishing is a linear function of F_y^D, $E_y^F = 6546.66F_y^D$, and days traveling is a linear function of days fishing, $E_y^T = 0.5021E_y^F$ (Poljak, 2013). Linear relationships between fishing mortality F_y^D and effort variables E_y^F and P_y^D are derived from an approximation $F_y^D \approx C_y/B_y$ and an assumption of cost-minimization with a Leontief (1941) production function for the relationship between effort variables $F_y^D = \text{Min}\left\{E_y^F/a_E, P_y^D/a_P\right\}$. Then, $F_y^D \approx C_y/B_y$ implies that catch is consistent with a Schaefer (1954) production function $C_y = B_y \times F_y^D$, which gives $C_y = B_y \times Min\left\{E_y^F/a_E, P_y^D/a_P\right\}$ where a_E, $a_P > 0$ are input coefficients and B_y is male mature biomass. Cost minimization with a Leontief production function implies that effort variables are used in fixed proportions $F_y^D = E_y^F/a_E = P_y^D/a_P$. The previous pair of equations imply $a_E = 6546.66$ (i.e., $E_y^F = 6546.66F_y^D$), and $a_P = 78.334 \times 6546.66$ (i.e., $P_y^D = 78.334E_y^F$).

2.4. Model projections

The model projections are undertaken for a range of values for fishing mortality (and hence effort), with fishing mortality assumed to be constant into the future. The parameters determining growth, natural mortality for post-recruit animals, costs and prices are set to the estimates for the last year of the assessment period. The base model for the analyses of this paper involves assuming that recruitment is governed by Eq. (13a). However, the sensitivity of relationships among MMB, effort, catch and profit to the use of Eq. (13b) is explored for the case of deterministic dynamics.

The bulk of the analyses of this paper are based on the assumption $\sigma_R = 0$ (Eq. (13)). The implications of stochasticity about the density-dependence function is examined by projecting the population forward where the extent of variation in recruitment about Eq. (13) is based on the empirical variation about Eqs. (13a) and (13b) when they are fitted to data (Table B.5). The yield in 100 years as a function of the fully-selected exploitation rate for the directed pot fishery is then summarized by quantiles of the probability distribution for yield conditioned on fully-selected exploitation rate. Projections are undertaken for projection years 2010 to 2109. These projections are based on the assumption that density-dependence occurs when the embryos are produced (equivalent to the mature male biomass at the time of spawning) and that adult natural mortality equals its value in the last year for which data are available (natural mortality is assumed constant in the assessment since the mid-1980s in the absence of information to suggest otherwise).

3. Results

3.1. Parameter estimation

Fig. 3 shows the fit of the best fit linear (i.e., $\phi_S = 1$; γ estimated) and non-linear (i.e., ϕ_S and γ estimated) models to the Kodiak experimental data. The linear model fits the data for pH = 7.5 well (Fig. 3c) (both models are tuned to the data for pH = 8.0 so the fits in Fig. 3a for these two cases are identical), but substantially under-predicts survival for pH = 7.8 (Fig. 3b). In contrast, the best

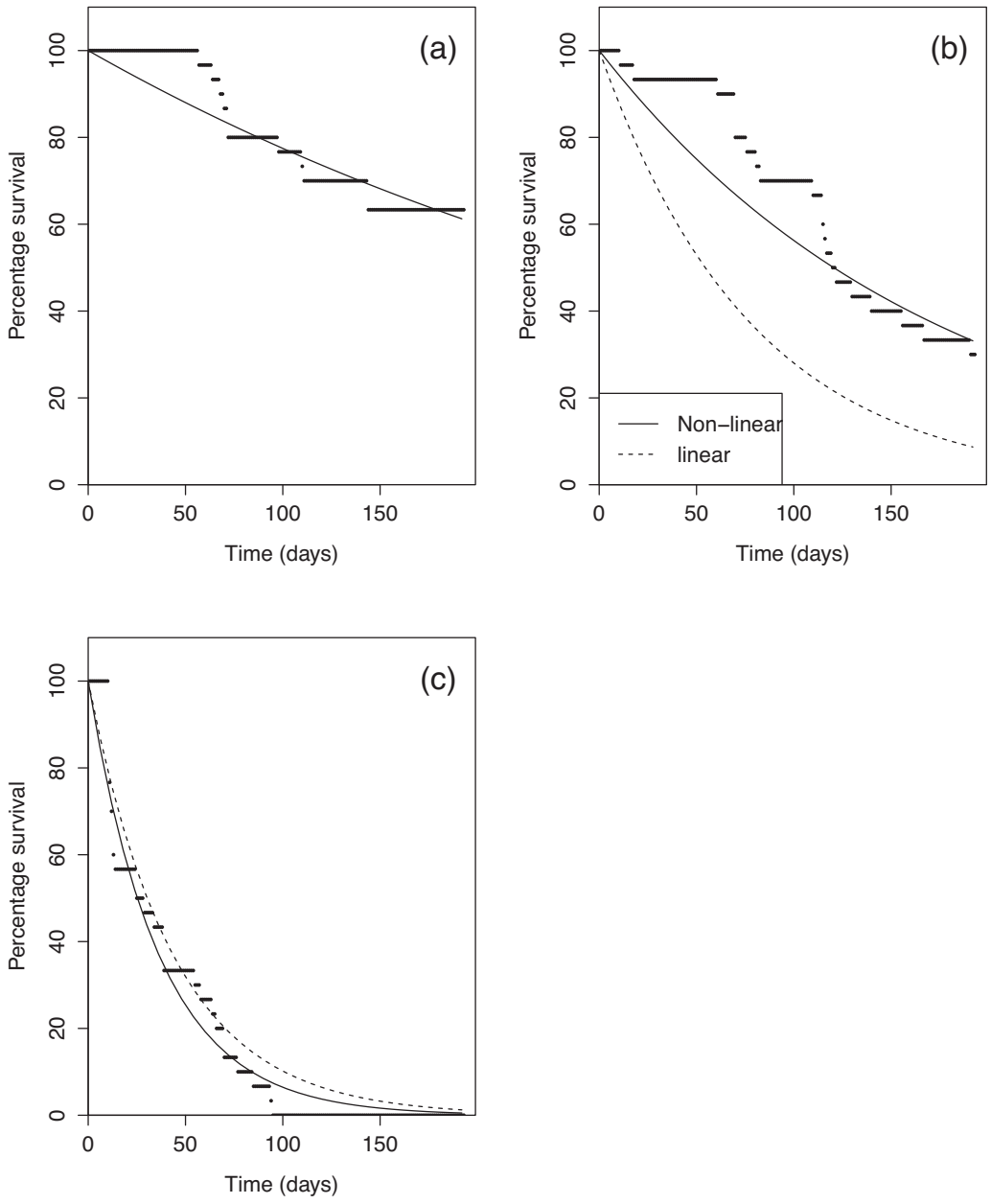

Fig. 3. Observed survival rates for the Kodiak experiment (dots) and best linear ($\phi_S = 0$) and non-linear (ϕ_S estimated) models. Results are shown for pH = 8.0, 7.8, and 7.5 in panels a–c, respectively.

fit non-linear model ($\gamma = -1399.26$; $\phi_S = 2.964$), fits the data set for pH = 7.8 much better. It should be noted that even the non-linear model is unable to mimic the relatively high survival rates for the first 50 days for the two highest values for pH (Fig. 3a and b). Fig. 4a shows a bootstrap distribution for survival over the first 192 days under control conditions, which suggests that survival under the control is not very well defined (90% interval 0.5–0.77), owing to the small number of animals in the experiment. The distribution for the parameter γ is very skewed (Fig. 4b [90% interval: −7246.42; −297.15]), while that for the power parameter, ϕ_S, is less skewed (90% interval: 2.340; 3.528) (Fig. 4c). Fig. 5 shows the bootstrap distributions for the percentage of embryos which survive to recruit, indicating bootstrap 50% and 90% intervals for embryos spawned over a 100 year projection period. The variance in survival at age is highest between years 40 and 60. Given that the power function fits the data appreciably (and statistically) much better than the linear fit, all subsequent analyses are based on the model in which ϕ_S and γ are estimated.

The population dynamics model was fitted to a variety of data sources (Appendix B). However, the focus for the evaluation of the ability of the model to adequately reproduce the available data is on the ability to mimic the abundance indices (Fig. 6). The model captures the trend in the abundance indices from the NMFS trawl survey, but there is some evidence for model misspecification (relatively long sequences of positive then negative residuals) (Fig. 6, left panel). The model matches the 2007 index from the BSFRF survey almost exactly, but is unable to match that for 2009 (Fig. 6, right panel). The patterns of residuals are consistent with those for the actual assessment (e.g., Zheng and Siddeek, 2011). Although not shown in Fig. 6, the model is also able to adequately mimic the catches and the survey and fishery length–frequency data.

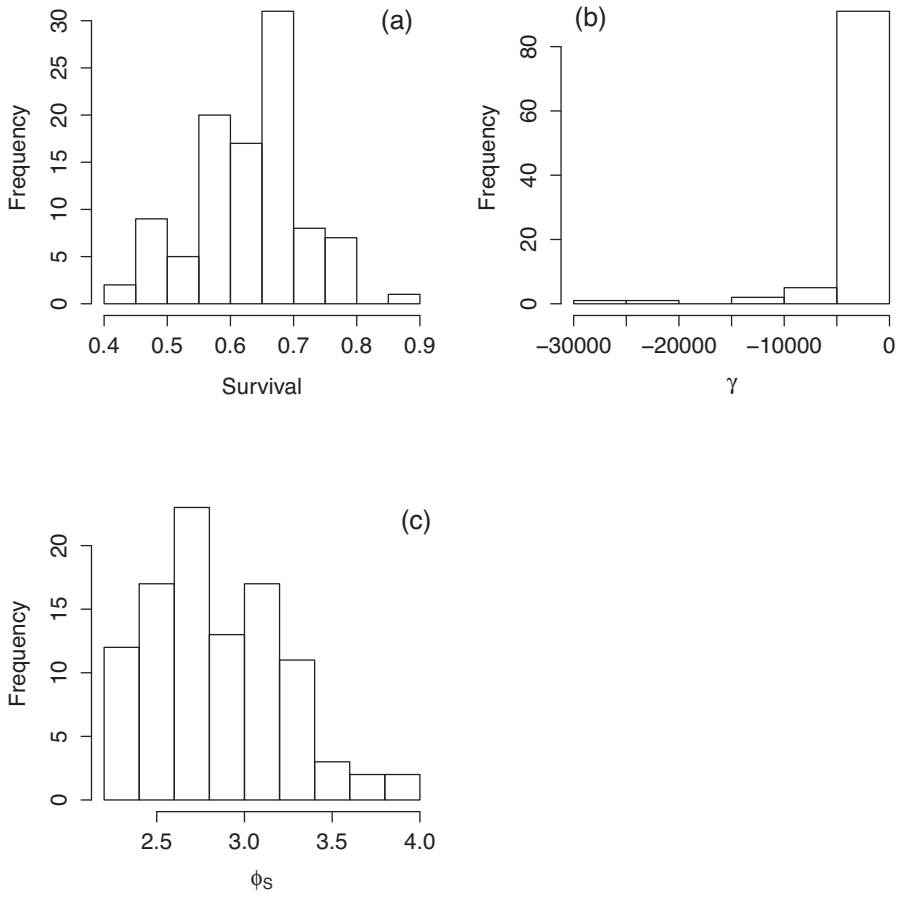

Fig. 4. Bootstrap distributions for the proportion of the juvenile crab surviving to 192 days under control conditions, and those for the γ and ϕ_S parameters of the non-linear model.

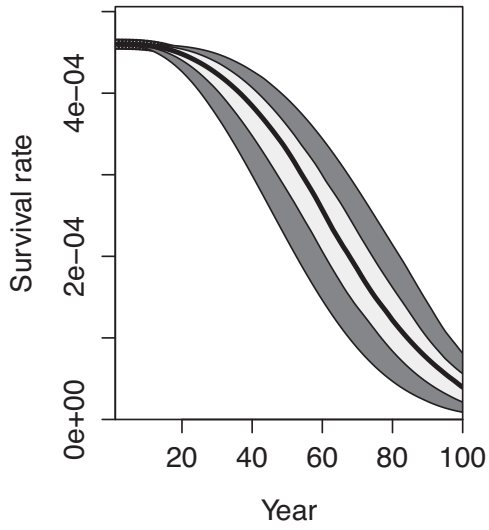

Fig. 5. Bootstrap distributions for the percentage of embryos which subsequently recruit to the first stage in the post-recruit model as a function of time since the present (the shaded areas cover 90% and 50% of the distributions; the solid line is the median).

3.2. Yield and profit in the absence of OA

The value for MMB_{MSY}, the biomass corresponding to MSY, as well as the effort and exploitation rate at which MSY is achieved, are the same for Eqs. (13a) and (13b) given that h and R_0 are computed so that $F_{MSY} = F_{35\%}$ and B_{MSY} equals the value specified by the NPFMC Scientific and Statistical Committee. However, MMB_{MSY} relative to MMB_0 (unfished mature male biomass) differs between Eqs. (13a) and (13b) [lower under Eq. (13b) relationship] (Fig. 7a). This arises because the yield function is less symmetric under Eq. (13b) than under Eq. (13a).

The MEY is essentially the same for Eqs. (13a) and (13b) (Fig. 7d), which is not surprising given the similarity of the yield curves close to their maxima (Fig. 7a,b). However, bionomic equilibrium (the point at which costs equal revenues, and hence the point at which profit is zero), differs between Eqs. (13a) and (13b) (Fig. 7c and d). Fig. 8a shows the relationship between the probability distributions for yield and the fully-selected exploitation rate by the directed pot fishery when there are no OA impacts. As expected (e.g., Clark, 1993), the maximum of the yield function is lower when there is stochasticity (by 8.2%). The variation in yield as a function of exploitation rate is greatest for the effort levels close to those at which MSY is achieved. Variation in yield about its expected value declines over time (Fig. 8b–d), but the coefficient of variation in yield is approximately constant.

3.3. Yield and profit with OA

The upper panels of Fig. 9 illustrate the deterministic relationships between the pre-recruit survival (relative to that in the absence of OA-related increases in mortality)[2] and MSY, MEY and

[2] Stochastic yield functions are shown for 20, 40 and 60 years into the future in Fig. 6(b–d).

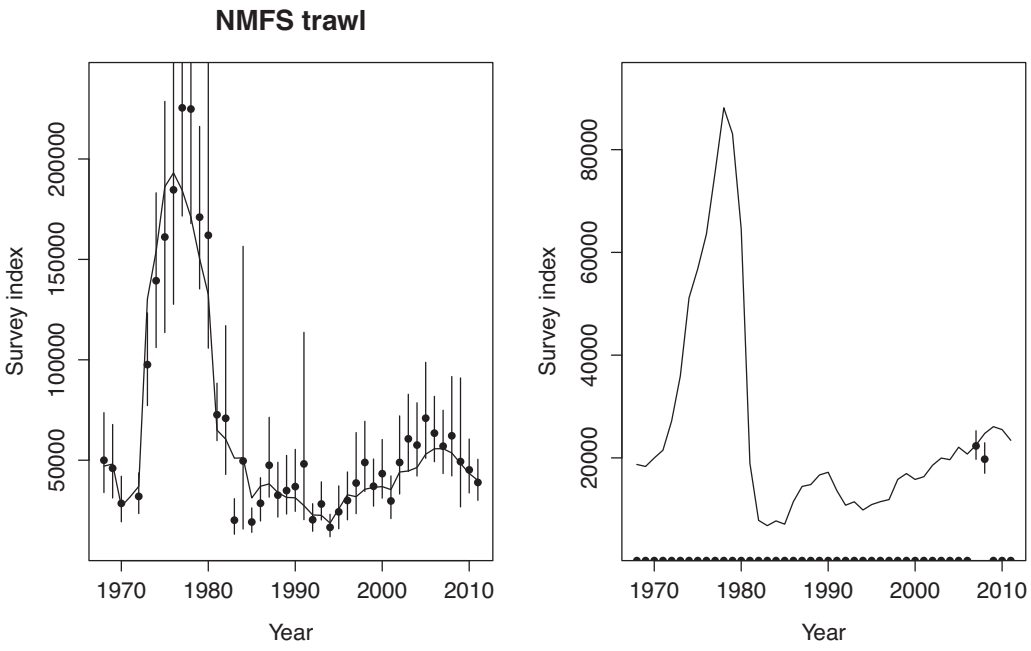

Fig. 6. Observed (solid dots) and model fits (lines) to the historical NMFS (left panel) and the BSFRF (right panel) surveys.

the efforts which maximize yield and profit. As expected, MSY and MEY decline with reductions in pre-recruit survival. MEY is zero at higher pre-recruit survival rates (and hence fewer years into the future) than MSY because costs depend on the exploitation rate in the directed pot fishery (Fig. 7c). Similarly, the effort which maximizes yield is higher than that which maximizes profit for all levels of pre-recruit survival. The value for $F_{35\%}$ declines with reductions in pre-recruit survival and equals zero for survival rates of 0.38 and

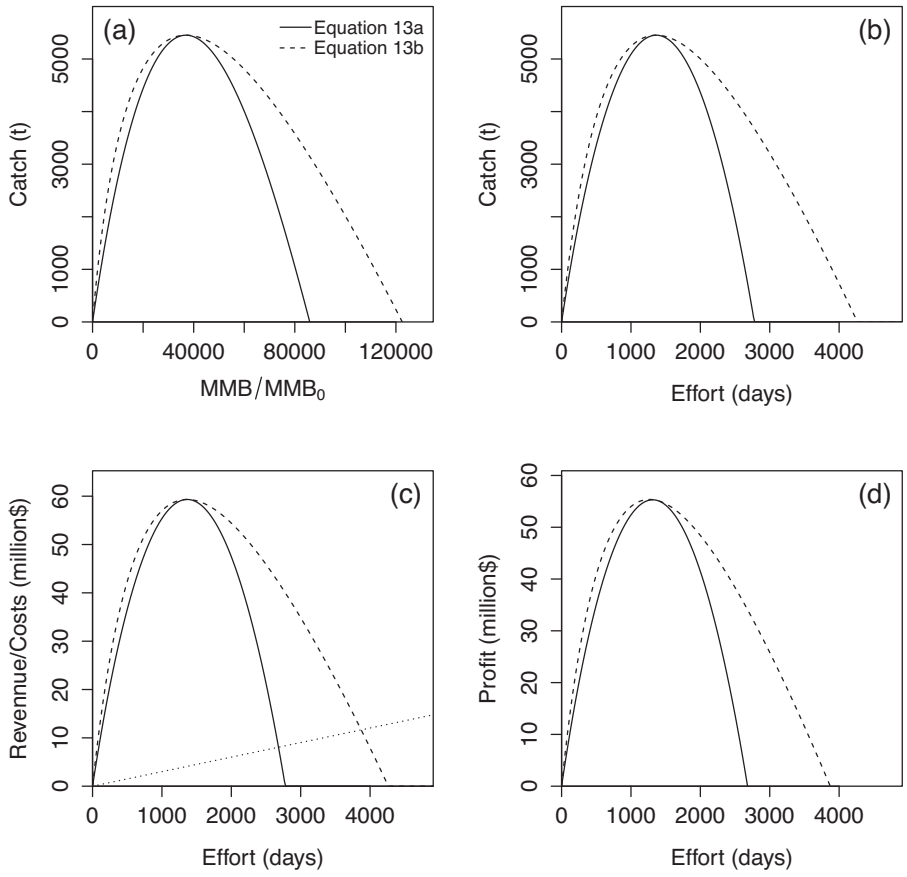

Fig. 7. Yield versus MMB relative to the unfished level (i.e., MMB/MMB_0) expressed as a percentage and versus effort, under deterministic conditions (a,b), revenue (solid and dashed lines) and cost (dotted line) versus effort (c), and profit versus effort (d). Results are shown for Eqs. (13a) and (13b). The results in the figure ignore OA impacts.

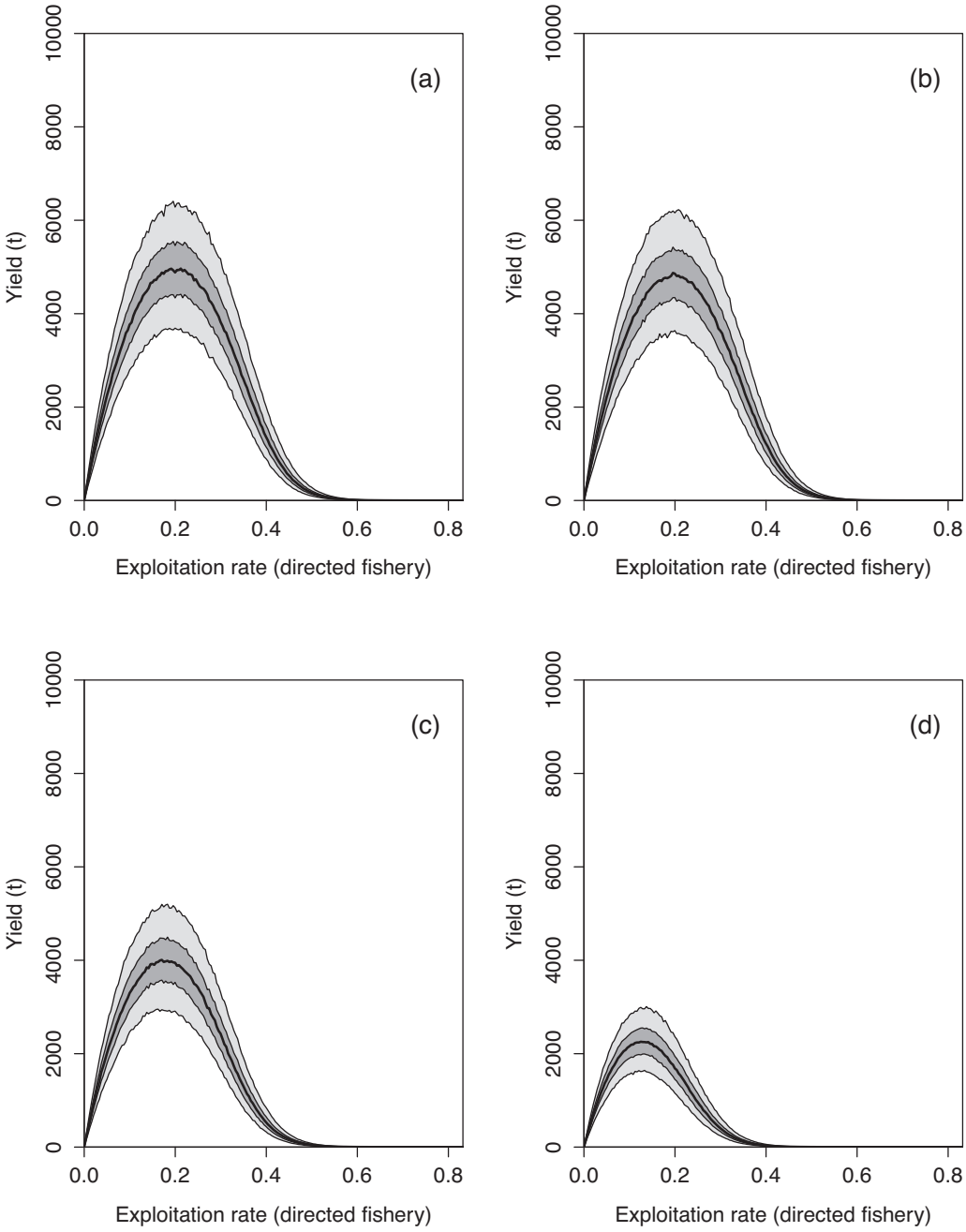

Fig. 8. Sensitivity of the relationship between fully-selected exploitation rate due to the directed fishery and yield when there is stochasticity about Eq. (13a) (light shared 90% interval; dark shared 50% interval; solid line median). Results are shown for the present (a), and 20, 40 and 60 years into the future under ocean acidification (b–d).

less. $F_{35\%}$ is zero because even under no harvest it is not possible to keep spawning biomass-per-recruit at 35% of unfished levels.

Fig. 10 shows similar results as Fig. 9, except that results are shown as a function of time rather than of relative survival rate. As expected, the yield and profit functions shift to "the left" (population collapses and MSY/MEY occur at lower levels of effort) and "down" (MSY and MEY are lower into the future) over the next 100 years (Fig. 10b and d). Similarly, the relationship between yield and MMB shifts to "the left" and "down" over time (Fig. 10c), implying that not only is yield lower into the future, but the average expected size of the stock in the absence of exploitation is lower. The relationship between expected survival and time is not linear (Fig. 10a), which leads MSY and MEY to not decline linearly over time but to remain fairly constant over the next 20-odd years before declining to zero by the end of 21st century (Fig. 10e and f). This result is a consequence of the relationship between survival rate and time which only declines slowly over the first 20 years of the projection period (Fig. 10a). The relationships between the efforts at which MSY and MEY occur and time (Fig. 10g) are not the same as that between $F_{35\%}$ and time (Fig. 10h). This is because $F_{35\%}$ is equal to F_{MSY} only in the absence of OA.

Fig. 10 is based on the best estimate of the relationship between pre-recruit survival and time. However, that relationship is uncertain, and Fig. 11 quantifies this uncertainty using a bootstrap procedure (see the bootstrap distributions in Fig. 4). Conducting projections in which allowance is made for variation in pre-recruit

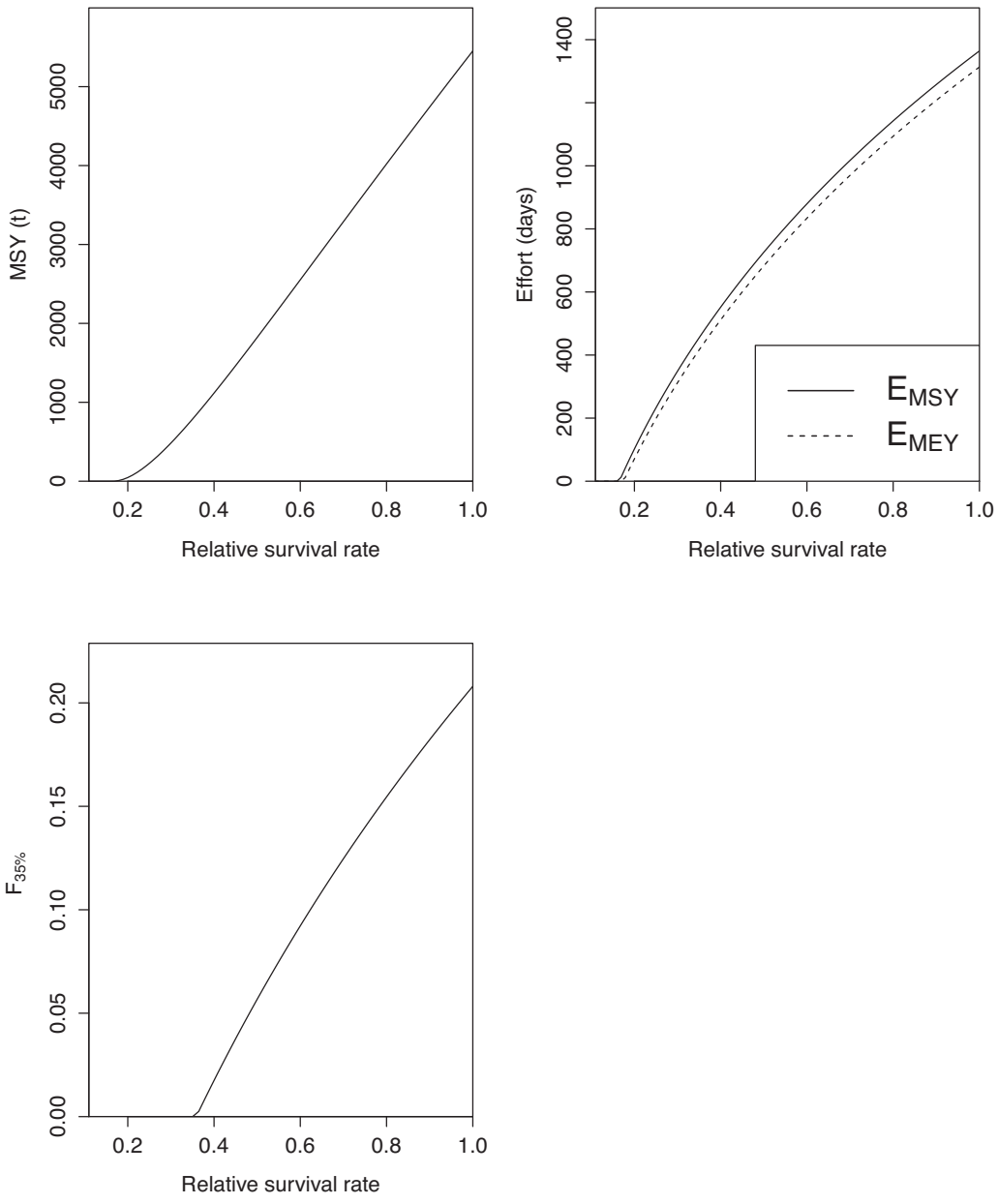

Fig. 9. Relationships between MSY, effort, and $F_{35\%}$, and the survival rate of pre-recruit crab relative to that in a non-OA situation. The solid and dashed lines for effort in the upper right panel respectively denote the effort levels which maximize long-term catch and profit.

survival leads to uncertainty in the values for key reference points and time (Fig. 10b–d). This uncertainty is lowest for the earliest years of the projection period, but increases over time and leads, for example, to quite considerable uncertainty in the years in which E_{MSY}, E_{MEY}, and $F_{35\%}$ are first zero.

4. Discussion

The model and estimation framework outlined in this paper provides a way to link scenarios related to trends in the physiological effects of ocean pH with recruitment to the model for the dynamics of crab which are surveyed and subject to a fishery. The linked pre- and post-recruit models together, incorporated into a bioeconomic model, provide a way to examine the effects of changes in ocean pH on yields and revenues from the fishery. The reference levels for the parameters of the model which determine growth and survival are set based on past field and laboratory studies, while the parameters which link ocean pH and survival are based on the more recent results of the experiments conducted at the NMFS Kodiak laboratory for Bristol Bay red king crab.

There are several ways in which the approach outlined in this paper could be improved. First, the amount of data from the experiments conducted at the Kodiak laboratory is limited by sample size (only 30 individuals at each pH), which means that estimated survival rates are fairly imprecise (Fig. 4, upper left panel). Additional data will help to better characterize the relationship between pH and survival. Furthermore, the initial experiments available for this modeling work only provided information on the juvenile life history stage. Subsequent experimental results recently published (Long et al., 2013b) provide data on the impact of pH on embryogenesis and on survival and growth of the larval stages which could be included in future analyses by making f_i a (decreasing) function of time.

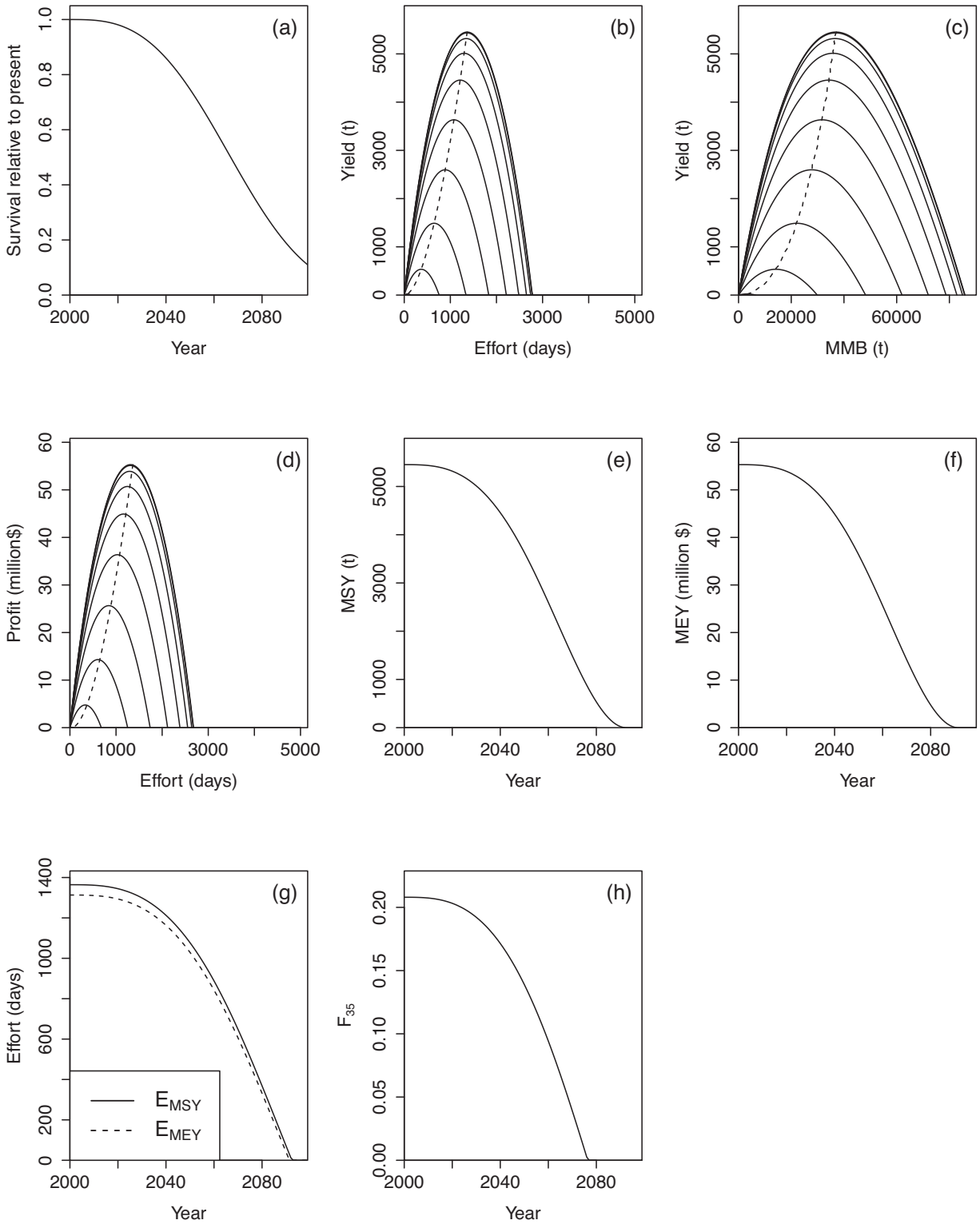

Fig. 10. Outputs from deterministic projections under the Beverton-Holt stock recruitment relationship for a range of future years, illustrating the impact of ocean acidification on the yield and profit functions, as well as on MSY, MEY E_{MSY}, E_{MEY}, and $F_{35\%}$.

Notwithstanding the relatively small sample sizes for model calibration, there is evidence for model mis-specification for pH values of 8.0 and 7.8 (Fig. 3b and c) which could be resolved by adopting a more general (e.g. "hazard" or "half normal") functional form for the relationships between pH and survival/stage duration, although this would not impact the qualitative conclusions of the study. Another concern with the model is that allowing for changes over time in survival, while keeping the length of time in a stage constant, implies that the values for the $P_{i,T}$ are lower when survival is lower.

The survival rates for the no-OA scenario were tuned to the results for the control from the Kodiak experiments (Fig. 3a). However, those experiments did not (could not) assess the impact of OA on ecosystem functions such as predation rates or prey availability,

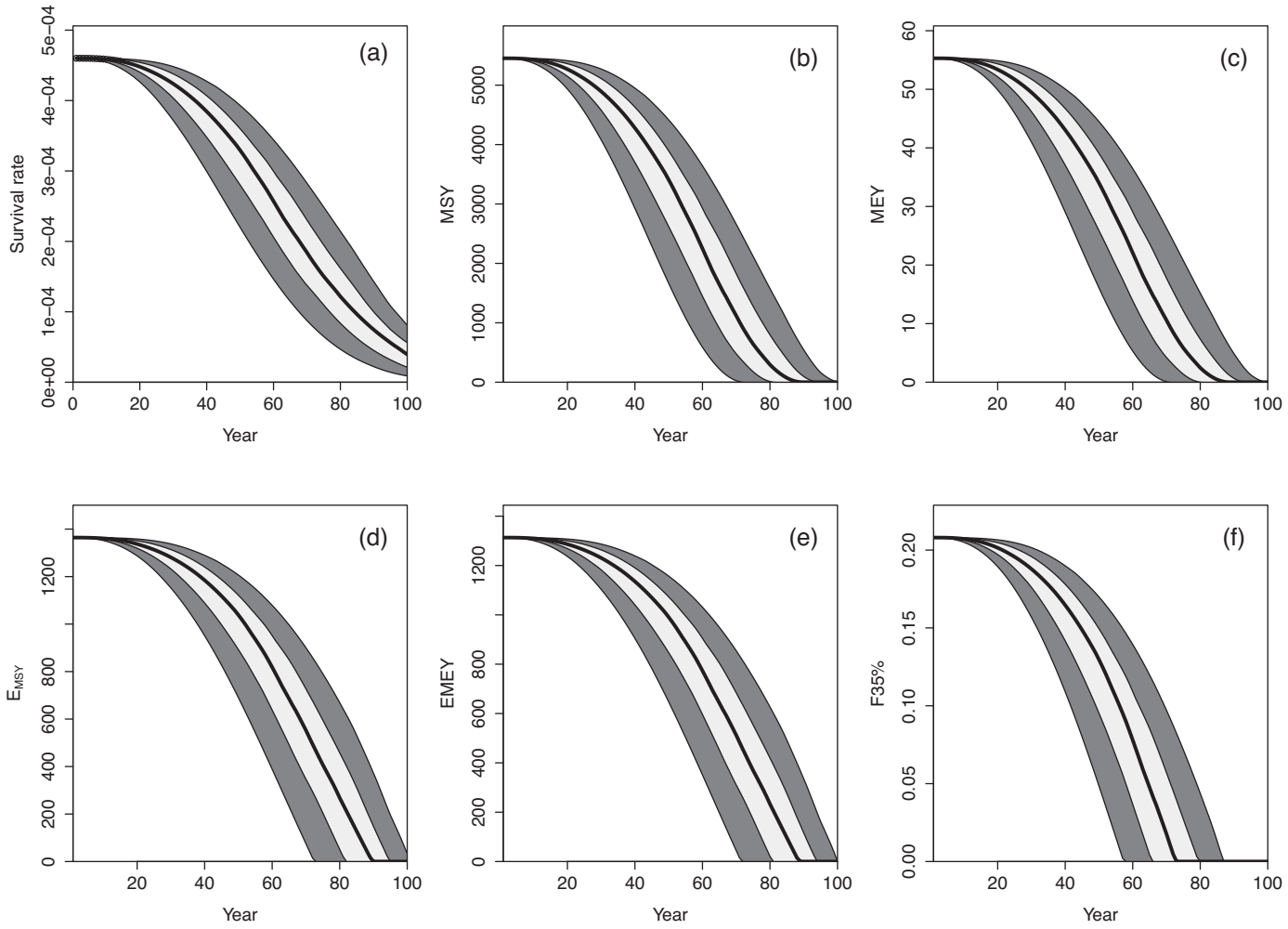

Fig. 11. Pre-recruit survival rate, MSY, MEY, E_{MSY}, E_{MEY} and $F_{35\%}$ for Bristol Bay red king crab versus time. The solid shading denotes 90% intervals, the light shading 50% intervals, and the solid line the medians.

for example. Consequently, the experimental estimates of survival, even for the controls, are likely under-estimates. In relation to OA impacts, the experiments did not examine the joint effects of likely changes in temperature and pH on survival rates. However, the experiments may overestimate mortality due to OA and changes in average temperatures if adaptation takes places. The Kodiak experiments involved major changes in pH, and slower changes may lead to adaptation, reducing the extent to which mortality increases with OA. Finally, the experiments were conducted under relatively constant pH levels. However, it likely that pH levels will vary on various scales: diurnal (due to local phytoplankton production), seasonal (due to production or upwelling events), and interannual (due to changes in current structure forced by climatic conditions). Data on in situ pH variability and experimental designs which reflect this variation, would further enhance the data available to parameterize models of the impact of OA on pre-recruit red king crab.

The relationship between time and future pH is assumed to be linear. Given the illustrative nature of our analyses, the exact time-series of changes in pH will impact the quantitative, but not the qualitative, conclusions of this study, justifying the use of a simple relationship. Future analyses could improve upon this simple relationship by utilizing spatial OA projections from coupled regional-global oceanographic models for the Bering Sea, for example.

Although yield curves are traditionally computed under the assumption of deterministic dynamics (e.g. Fig. 7), the impact of stochasticity in recruitment (and potentially natural mortality and growth) means that the actual catch (and profit) will differ (perhaps markedly) from the deterministic expectation. The extent of variation in yield due to recruitment variation is quantified by setting σ_R based on the fit of Eqs. (13a) and (13b). Accounting for this variation is important because the model predicts that the deterministic effects of OA on biomass and productivity will be swamped by natural variation for several decades.

The relationships between expected yield and profit and effort are not predicted to change much over time given the predicted relationship between survival and OA (and hence time). However, the fit of the model relating survival and time is relatively poor for high pH values. The results of the long-term projections should therefore be interpreted with caution until further experiments are conducted. The results in Fig. 6 ignore error due to variation about the density-dependence function as well as that due to uncertainty in the parameters which determine the relationship between survival and time (e.g., Fig. 11). A next step in this modeling work would be to integrate all the sources of uncertainty into a single analysis which would then provide a way to estimate how long it is likely to be before it will be possible to detect a change in catch given those uncertainties which can be reduced due to additional sampling such as uncertainties regarding selectivity parameters

and those which are unresolvable as they relate to future values for quantities such as the variation about Eq. (13) which depend on factors such as future environmental conditions.

The rate at which $F_{35\%}$ drops over time (Fig. 10h) is faster than the rate at which F_{MSY} drops over time (Fig. 10g) even though $F_{MSY} = F_{35\%}$ in the absence of OA. This arises because $F_{35\%}$ and F_{MSY} are defined differently. Specifically, $F_{35\%}$ is defined as the fully-selected exploitation rate by the directed pot fishery such that the fraction of animals which survive fishing is 35% of that in the absence of both exploitation and OA, while F_{MSY} is the fully selected exploitation rate by the directed pot fishery at which yield is maximized given OA. The difference in values arises because the density-dependence function is assumed to be static and not to change due to OA. Whether this assumption is valid depends on what drives density dependence. It is not implausible, for example, that OA could reduce the resilience of the population, which would reduce F_{MSY} in each future year more rapidly. In contrast, the density-dependence function may be unchanged under OA (this is the assumption underlying the analyses of this paper) if density dependence is related to finding shelter after settlement. The results would be sensitive to when in the life-cycle density-dependence occurs. If density-dependence occurs during the adult stage rather than during the pre-recruit stage, the impact of OA will be substantially less. However, density-dependence is likely to occur during the pre-recruit phase due for example to starvation and predation during the pelagic and early benthic stages.

This study is a first step toward a fully-integrated understanding of the impacts of OA on fishery yields and profits. There is a shortage of studies on the impacts of OA on society, and the models employed for analysis in these studies are in an early stage of development (Malakoff, 2012). Griffith et al. (2011) and Kaplan et al. (2010) explored the impacts of OA on fished systems using ecosystem models. Those studies were able to more fully explore impacts such as those on predation and foodweb structure and ultimately on biomass and yield. The model of this paper explored the impact of OA for a single species using a detailed model of pre- and post-recruit dynamics. It was also fitted to data on OA impacts on survival and fishery impacts on biomass and length-structure. As such, the model is an example of a Model of Intermediate Complexity for Ecosystem Assessments, MICE (Plagányi et al., 2014). The model of post-recruit dynamics also closely resembles that used for management purposes and is able to produce the types of outputs used directly for fisheries management. Detailed single-species models, ecosystem models and experiments (field and lab) complement each other and will be necessary for managers as they plan responses to OA.

The comparison of outcomes for a simple OA scenario to those without OA effects, based on two types of objectives for management, maximizing profits, and maximizing yields show that yields and profits for the Bristol Bay red king crab fishery are projected to decline, gradually for the next few decades, and then, experience a more severe impact after 2050. Direct losses to the commercial fishery may be substantial in the future, on the order of tens of millions of dollars per year. The indirect costs of OA could be much larger because commercial fishing is an important economic sector in the state of Alaska. Estimates of indirect economic impacts associated with OA are needed. Similar studies to this one for other Alaska crab stocks are a high priority for future research.

Acknowledgements

AEP and DP were supported by NOAA through the NOAA Ocean Acidification Program. Martin Dorn (AFSC, NOAA), the editor and two anonymous reviewers are thanked for their comments on an earlier version of this paper. The findings and conclusions in the paper are those of the authors and do not necessarily represent the views of the National Marine Fisheries Service.

Appendix A. Derivation of Eq. (3)

Let S be the survival rate for a given stage, n be the minimum number of time-steps that an animal needs to be in the stage before it can move to the next step, and p be the probability of moving to the next stage each time-step once an animal has been in the stage for n time-steps (moving to the next stage is assumed to take place at the end of the time-step after survival). For the case $n = 3$, the dynamics of the stage can be written as:

$$\begin{pmatrix} 0 & 0 & 0 & 0 \\ S & 0 & 0 & 0 \\ 0 & S & S(1-p) & 0 \\ 0 & 0 & Sp & 1 \end{pmatrix} \begin{pmatrix} N_1 \\ N_2 \\ N_{3+} \\ \Omega \end{pmatrix} \tag{A.1}$$

where N_1, N_2, N_{3+} are the numbers of animals which have been in the stage for 1, 2 and 3+ time-steps, and Ω is the number of animals which have left the stage.

The number of animals leaving the stage are S^3p after 3 time-steps, $S^4(1-p)p$ after 4 time-steps, $S^5(1-p)^2p$ after 5 time-steps, etc. This is a geometric progression of the form $(S^3p(1+(1-p)S+(1-p)^2S^2..)$ which sums to:

$$\frac{S^3p}{1-(1-p)S} \tag{A.3}$$

Generalizing Eq. (A.3) from a minimum of 3 to n time-steps leads to Eq. (3).

The average time to leave a stage is:

$$\frac{\sum_{i=1} iN_{3+,i}Sp}{\sum_i N_{3+,i}Sp} \tag{A.4}$$

where $N_{3+,i}$ is the number of animals in the 3+ class at the start of time-step i.

Appendix B. The likelihood function for the post-recruit model

The values of the parameters of the post-recruit model are either estimated by fitting the model to the available data (Table B.1) or pre-specified (Table B.2). Table B.3 summarizes the data used to estimate the parameters.

The contribution of the catches to the negative of the logarithm of the likelihood function is given by:

$$L_1 = \lambda_1^{Da}\sum_y \left(ln\tilde{C}_y^D - ln\tilde{C}_y^{D,obs}\right)^2 + \lambda_1^{Db}\sum_y \left(ln\bar{C}_y^D - ln\bar{C}_y^{D,obs}\right)^2 + \lambda_1^T\sum_y \left(ln\bar{C}_y^T - ln\bar{C}_y^{T,obs}\right)^2 \tag{B.1}$$

where λ_j is a weighting factor (often by fleet; see Table B.4), $\tilde{C}_y^{D,\mathrm{obs}}$ is the observed retained pot catch during year y, $\bar{C}_y^{D,\mathrm{obs}}$ is the observed discarded pot catch during year y, and $\bar{C}_y^{T,\mathrm{obs}}$ is the observed discard by the trawl fishery.

The contribution of the length frequency data from the pot fishery to the negative of the logarithm of the likelihood function is

Table B.1
The estimable parameters of the population dynamics model.

Parameter	Number of parameters
Natural mortality	
M for 1976–1979; 1985–1993	1
M for 1980–1984	1
Transition matrix	4
Fishery selectivity	
Directed fishery (2 epochs; 1968–1972; 1973–2010)	6
Groundfish fisheries	4
Tanner crab fishery	4
Survey selectivity	
NMFS trawl survey (4 epochs; 1968–1969; 1970–1972; 1973–1981; 1982–2010)	20
BSFRF trawl survey	0 (selectivity is pre-specified)
Probability of retention	5
Survey catchability	
NMFS trawl survey (2 epochs; 1968–1969; 1970–2010)	2 (pre-specified for 1970–2010)
BSFRF trawl survey	1 (pre-specified)
Numbers-at-length at the start of 1968	5
Fishing mortality	
Directed fishery	40
Groundfish fishery	43
Tanner crab fishery	29
Recruitment	
Mean recruitment	1
Annual recruitment deviations	43

Table B.2
Values for the pre-specified parameters of the model (Poljak, 2013),.

	Length-class (mm)				
	65–80	80–100	100–120	120–140	140+
Weight, W_i (kg)	0.3265	0.6483	1.1795	1.9460	3.0429
Fecundity, f_i	0.0000	0.0000	0.3528	1.9460	3.0429

given by:

$$L_2 = -\lambda_2^{Da}\sum_y \tilde{N}_{D,y}^{Eff}\sum_i \tilde{\rho}_{y,i}^{D,obs} ln\left(\frac{\hat{\tilde{\rho}}_{y,i}^{D}}{\tilde{\rho}_{y,i}^{D,obs}}\right) - \lambda_2^{Db}\sum_y \tilde{N}_{0,y}^{Eff}\sum_i \bar{\rho}_{y,i}^{D,obs} ln\left(\frac{\hat{\bar{\rho}}_{y,i}^{D}}{\bar{\rho}_{y,i}^{D,obs}}\right) - \lambda_2^{f}\sum_y N_y^{T,Eff}\sum_i \rho_{y,i}^{T,obs} ln\left(\frac{\hat{\rho}_{y,i}^{T}}{\rho_{y,i}^{T,obs}}\right) \quad \text{(B.2)}$$

Table B.3
Summary of the data included in the post-recruit model.

Data type	Years
Catches	
Landings in the pot fishery	1968–2010
Discards in the pot fishery	1990–2010
Discard in the groundfish fisheries	1976–2010
Discard in the fishery for Tanner crab	1991–2010
Survey index data	
NMFS trawl survey	1968–1970; 1972–2010
BSFRF trawl survey	2007–2008
Effort data	
Tanner crab fishery	1968–1994
Catch/discard length–frequency data	
Landings in the pot fishery	1968–1982; 1984–1993; 1996–2010
Discards in the pot fishery	1990–1993; 1996–2010
Discard in the groundfish fisheries	1976–1992; 1994–2010
Discard in the fishery for Tanner crab	1991–1993
Survey length–frequency data	
NMFS trawl survey	1968–1970; 1972–2010

Table B.4
The factors used to weight the data included in the post-recruit model.

Data type	Weighting factor
Catches	
Landings in the pot fishery, λ_1^{Da}	100
Discards in the pot fishery, λ_1^{Db}	10
Discard in the groundfish fisheries, λ_1^{T}	10
Survey index data	
NMFS trawl survey	1
BSFRF trawl survey	1
Catch/discard length–frequency data	
Landings in the pot fishery, $\lambda_2^{Da}\tilde{N}_y^{D,Eff}$	Actual sample size scaled with a maximum of 200
Discards in the pot fishery, $\lambda_2^{Db}\tilde{N}_y^{D,Eff}$	Actual sample size scaled with a maximum of 20
Discard in the groundfish fisheries, $\lambda_2^{T}N_y^{T,Eff}$	Actual sample size scaled with a maximum of 20
Survey length–frequency data	
NMFS trawl survey, $\lambda_3 N_y^{I,Eff}$	400

Table B.5
Values for the parameters of the density-dependence functions estimated by fitting these functions to the outputs from the stock assessment.

Parameter	Value
Unfished recruitment, R_0	
Eq. (13a)	11,168 millions
Eq. (13b)	16,136 millions
Steepness, h	
Eq. (13a)	0.862
Eq. (13b)	0.760
σ_R	
Eq. (13a)	0.6787
Eq. (13b)	0.6729

where $N_{i,y}^{Eff}$ is the effective sample size for data-type i (Table B.4), $\tilde{\rho}_{y,i}^{D,obs}$, $\bar{\rho}_{y,i}^{D,obs}$ and $\rho_{y,i}^{T,obs}$ are respectively the observed proportion of the catch retained during the directed fishery, discarded during the directed fishery and discarded in the trawl fishery during year y which is in length-class i, and $\hat{\tilde{\rho}}_{y,i}^{D}$, $\hat{\bar{\rho}}_{y,i}^{D}$ and $\hat{\rho}_{y,i}^{T,obs}$ are respectively the model-estimates corresponding to $\tilde{\rho}_{y,i}^{obs}$, $\bar{\rho}_{y,i}^{obs}$ and $\rho_{y,i}^{T,obs}$:

$$\hat{\tilde{\rho}}_{y,i}^{D} = \frac{\tilde{C}_{y,i}^{D}}{\sum_i \tilde{C}_{y,i}^{D}} \quad \hat{\bar{\rho}}_{y,i}^{D} = \frac{\bar{C}_{y,i}^{D}}{\sum_i \bar{C}_{y,i}^{D}} \quad \hat{\rho}_{y,i}^{T} = \frac{\bar{C}_{y,i}^{T}}{\sum_i \bar{C}_{y,i}^{T}} \quad \text{(B.3)}$$

The contribution of the survey data (NMFS survey and Bering Seas Fisheries Research Foundation [BSFRF]) to the negative of the logarithm of the likelihood function is given by:

$$L_3 = 0.5\sum_y \frac{(\ln I_y - \ln \hat{I}_y)^2}{2[\sigma_y^I]^2} - \lambda_3\sum_y N_y^{I,Eff}\sum_i \rho_{y,i}^{I,obs} \ln\left(\frac{\hat{\rho}_{y,i}^{I}}{\rho_{y,i}^{I,obs}}\right) \quad \text{(B.4)}$$

where I_y is the survey index for year y, σ_y^I is the standard error of the logarithm of I_y, $\hat{I}_y$ is the model-estimate corresponding to I_y:

$$I_y = \sum_y J_{y*,i}^{I} N_{y,i} \quad \text{(B.5)}$$

$J_{y*,i}^{I}$ is survey selectivity for year y (where year y falls within one of a number of epochs, y^*; Table B.1), $\rho_{y,i}^{I,obs}$ is the observed proportion of the survey catch by survey type I during year y which is in length-class i, and $\rho_{y,i}^{I}$ is the model-estimate of the proportion

of the survey catch by survey type I during year y which is in length-class i:

$$\rho^I_{y,i} = \frac{S^I_{y*,i} N_{y,i}}{\sum_j J^I_{y*,j} N_{y,j}} \quad \text{(B.6)}$$

Penalties are placed on the deviations of log-recruitment from mean log-recruitment as well as on the deviations in fishing mortality from mean fishing mortality, i.e.:

$$P = \lambda_4 \sum_y \varepsilon_y^2 + \sum_f \lambda_5^f \sum_y \left(F_y^f - \bar{F}^f\right)^2 \quad \text{(B.7)}$$

where $\bar{F}^f$ is the mean over the F_y^f (for the years in which $F_y^f \neq 0$). The values for λ_4 and λ_5^f are set to 1 and 0.001, respectively. Catchability for the NMFS trawl survey is set to 0.896 and that for the BSFRF survey is assumed to 1 consistent with the actual stock assessment for BBRKC. The selectivity pattern for the BSFRF survey is pre-specified (J. Zheng, pers. commn).

References

Armstrong, D.A., Incze, L.S., Wencker, D.L., Armstrong, J.L., 1981. Distribution and abundance of decapod crustacean larvae in the southeastern Bering Sea with emphasis on commercial species. U.S. Dep. Commer., NOAA, OCSEAP Final Rep. 53 (1986), 79–878.

Caldeira, K., Wickett, M.E., 2003. Anthropogenic carbon and ocean pH. Nature 425, 365-365.

Ceballos-Osuna, L., Carter, H.A., Miller, N.A., Stillman, J.H., 2013. Effects of ocean acidification on early life-history stages of the intertidal porcelain crab *Petrolisthes cinctipes*. J. Exp. Biol. 216, 1405–1411.

Cooley, S.R., Doney, S.C., 2009. Anticipating ocean acidification's economic consequences for commercial fisheries. Environ. Res. Lett. 4 (June), 024007, http://dx.doi.org/10.1088/1748-9326/4/2/024007.

Clark, W.G., 1993. The effect of recruitment variability on the choice of a target level of spawning biomass per recruit. In: Kruse, G., Marasco, R.J., Pautzke, C., Quinn II, T.J. (Eds.), Proceedings of the International Symposium on Management Strategies for Exploited Fish Populations. University of Alaska, Alaska Sea Grant College Program Report 93-02, Fairbanks. , pp. 233–246.

Donaldson, W.E., Beyersdorfer, S.C., Pengilly, D., Blau, S.F., 1992. Growth of red king crab, *Paralithodes camtschaticus* (Tilesius, 1815), in artificial habitat collectors at Kodiak, Alaska. J. Shellfish Res. 11, 85–89.

Doney, S.C., Fabry, V.J., Feely, R.A., Kleypas, J.A., 2009. Ocean acidification: the other CO_2 problem. Ann. Rev. Mar. Sci. 1, 169–192.

Efron, B., 1982. The Jacknife, the Bootstrap, and Other Resampling Plans. CBMS-NSF, Philadelphia.

Fabry, V.J., McClintock, J.B., Mathis, J.T., Grebmeier, J.M., 2009. Ocean acidification at high latitudes: The bellweather. Oceanography 22, 160–171.

Feely, R.A., Sabine, C.L., Lee, K., Berelson, W., Kleypas, J., Fabry, V.J., Millero, F.J., 2004. Impact of anthropogenic CO_2 on the $CaCO_3$ system in the oceans. Science 305, 362–366.

Francis, R.I.C.C., 1992. Use of risk analysis to assess fishery management strategies: a case study using orange roughy (*Hoplostethus atlanticus*) on the Chatham Rise, New Zealand. Can. J. Fish. Aquat. Sci. 49, 922–930.

Garber-Yonts, B., Lee, J., 2012. Stock Assessment and Fishery Evaluation Report for King and Tanner Crab Fisheries of the Bering Sea and Aleutian Islands regions: 2012 Economic Status Report. Alaska Fisheries Science Center, Seattle, WA, pp. 145.

Griffith, G.P., Fulton, E.A., Richardson, A.J., 2011. Effects of fishing and acidification-related benthic mortality on the southeast Australian marine ecosystem. Glob. Chang. Biol. 17, 3058–3074.

Hall-Spencer, J.M., Rodolfo-Metalpa, R., Martin, S., Ransome, E., Fine, M., Turner, S.M., Rowley, S.J., Tedesco, D., Buia, M.C., 2008. Volcanic carbon dioxide vents show ecosystem effects of ocean acidification. Nature 454, 96–99.

Kaplan, I.C., Levin, P.S., Burden, M., Fulton, E.A., 2010. Fishing catch shares in the face of global change: a framework for integrating cumulative impacts and single species management. Can. J. Fish. Aquat. Sci. 67, 1968–1982.

Kovatcheva, N., Epelbaum, A., Kalinin, A., Borisov, R., Lebedev, R., 2006. Early Life History Stages of the Red King Crab *Paralithodes camtschaticus* (Tilesius 1815): Biology and Culture. VNIRO Publishing, Moscow.

Kurihara, H., Matsui, M., Furukawa, H., Hayashi, M., Ishimatsu, A., 2008. Long-term effects of predicted future seawater CO_2 conditions on the survival and growth of the marine shrimp *Palaemon pacificus*. J. Exp. Mar. Biol. Ecol. 367, 41–46.

Leontief, W., 1941. The Structure of the American Economy, 1919–1939. Oxford University Press, Oxford, UK.

Loher, T., Armstrong, D.A., Stevens, B.G., 2001. Growth of juvenile red king crab (*Paralithodes camtschaticus*) in Bristol Bay (Alaska) elucidated from field sampling and analysis of trawl-survey data. Fish. Bull. 9, 572–587.

Long, W.C., Swiney, K.M., Harris, C., Page, H.N., Foy, R.J., 2013a. Effects of ocean acidification on juvenile red king crab (*Paralithodes camtschaticus*) and Tanner crab (*Chionoecetes bairdi*) growth, condition, calcification, and survival. PLoS ONE 8 (4), e60959.

Long, W.C., Swiney, K.M., Foy, R.J., 2013b. Effects of ocean acidification on the embryos and larvae of red king crab *Paralithodes camtschaticus*. Mar. Pollut. Bull. 69, 38–47.

Malakoff, D., 2012. Researchers struggle to assess responses to ocean acidification. Nature 338, 27–28.

Mathis, J.T., Cross, J.N., Bates, N.R., 2011. The role of ocean acidification in the systemic carbonate mineral suppression in the Bering Sea. Geophys. Res. Lett. 38, L19602, http://dx.doi.org/10.1029/2011GL048884.

North Pacific Fishery Management Council (NPFMC), 2008. Amendment 24. Final Environmental Assessment for amendment 24 to the Fishery Management Plan for Bering Sea/Aleutian Islands King and Tanner Crabs to Revise Overfishing Definitions. North Pacific Fishery Management Council, 605 West 4th Ave, Anchorage, AK 99501.

Plagányi, É.E., Punt, A.E., Hillary, R., Morello, E.B., Thébaud, O., Hutton, T., Pillans, R.D., Thorson, J.T., Fulton, E.A., Smith, A.D.M., Smith, F., Bayliss, P., Haywood, M., Lyne, V., Rothlisberg, P.C., 2014. Multispecies fisheries management and conservation: tactical applications using models of intermediate complexity. Fish Fish. 15, 1–22.

Poljak, D., 2013. Impact of Ocean Acidification on Recruitment and Yield of Bristol Bay Red King Crab. University of Washington, (MS thesis).

Punt, A.E., Haung, T.-C., Maunder, M.N., 2013. Review of integrated size-structured models for stock assessment of hard-to-age crustacean and mollusc species. ICES J. Mar. Sci. 70, 16–33.

Punt, A.E., Siddeek, M.S.M., Garber-Yonts, B., Dalton, M., Rugolo, L., Stram, D., Turnock, B.J., Zheng, J., 2012. Evaluating the impact of buffers to account for scientific uncertainty when setting TACs: application to red king crab in Bristol Bay, Alaska. ICES J. Mar. Sci. 69, 624–634.

Punt, A.E., Szuwalski, C.S., Stockhausen, W., 2014. An evaluation of stock-recruitment proxies and environmental change points for implementing the US Sustainable Fisheries Act. Fish. Res. 157, 28–40.

Ries, J.B., Cohen, A.L., McCorkle, D.C., 2009. Marine calcifiers exhibit mixed responses to CO_2-induced ocean acidification. Geology 37, 1131–1134.

Schaefer, M.B., 1954. Some aspects of the dynamics of populations important to the management of commercial marine fisheries. Bull. Inter-Am. Trop. Tuna Comm. 1, 25–26.

Steinacher, M., Joos, F., Frölicher, T.L., Plattner, G.-K., Doney, S.C., 2009. Imminent ocean acidification in the Arctic projected with the NCAR global coupled carbon cycle-climate model. Biogeosciences 6, 515–533.

Sumaila, U.R., Cheung, W.W.L., Lam, V.W.Y., Pauly, D., Herrick, S., 2011. Climate change impacts on the biophysics and economics of world fisheries. Nat. Clim. Change 1301, 449–456.

Weber, D.O., 1967. Growth of immature king crab *Paralithodes camtschatica*(Tilesius). Int. N. Pac. Fish. Comm. Bull. 21, 21–53.

Whiteley, N.M., 2011. Physiological and ecological responses of crustaceans to ocean acidification. Mar. Ecol. Prog. Ser. 430, 257–271.

Zheng, J., Siddeek, M.S.M., 2009. Bristol Bay red king crab stock assessment in fall 2009. In: NPFMC (North Pacific Fishery Management Council). 2009. Stock Assessment and Fishery Evaluation Report for the King and Tanner Crab Fisheries of the Bering Sea and Aleutian Islands Region: 2009 Crab SAFE. September 2009. North Pacific Fishery Management Council, Anchorage.

Zheng, J., Siddeek, M.S.M., 2010. Bristol Bay red king crab stock assessment in fall 2010. In: NPFMC (North Pacific Fishery Management Council). 2010. Stock Assessment and Fishery Evaluation Report for the King and Tanner Crab Fisheries of the Bering Sea and Aleutian Islands Region: 2010 Crab SAFE. September 2010. North Pacific Fishery Management Council, Anchorage.

Zheng, J., Siddeek, M.S.M., 2011. Bristol Bay red king crab stock assessment in fall 2011. In: NPFMC (North Pacific Fishery Management Council). 2011. Stock Assessment and Fishery Evaluation Report for the King and Tanner Crab Fisheries of the Bering Sea and Aleutian Islands Region: 2011 Crab SAFE. September 2011. North Pacific Fishery Management Council, Anchorage.